Automatic Corneal Nerve Fibre Detection for Diabetic Neuropathy Quantification

M.A. Dabbah[1]
m.a.dabbah@manchester.ac.uk
J. Graham[1]
jim.graham@manchester.ac.uk
I. Petropoulos[2]
ioannis.petropoulos@manchester.ac.uk
M. Tavakoli[2]
mitra.tavakoli@manchester.ac.uk
R.A. Malik[2]
rayaz.a.malik@manchester.ac.uk

[1] Imaging Sciences and Biomedical Engineering (ISBE)
The University of Manchester
Oxford Rd, Manchester, M13 9PT, UK

[2] Cardiovascular Research Group
The University of Manchester
Grafton St., Manchester, M13 9NT, UK

Abstract

Diabetic neuropathy is one of the most common long term complications of diabetes. Current assessment methods of diabetic neuropathy are not satisfactory. In contrast, recent research has shown that corneal confocal microscopy (CCM) image analysis has the potential of being the surrogate endpoint to assess and quantify neuropathy. But to be clinically useful, the analysis has to be automated. In this paper, we present a detection algorithm that extracts corneal nerve fibres from CCM images using a dual-model of foreground and background regions. The models work interactively through a logistic function in order to identify a corresponding nerve fibre region. The paper compares the performance of this algorithm with the performance of other well-know curvilinear detection methods using a dataset of CCM images with ground-truth obtained by expert annotation clinicians. The evaluation have shown a significant improvement ($p \approx 0$) in both error rates and signal-to-noise ratios over the competitor methods.

1 Introduction

Figures from recent international statistical reports [11] show an alarming increase of 54% in the global diabetic population by 2030, which brings the total number of adults with diabetes to 438.7 millions. In England for example [4], up to one in 20 people has diabetes and by 2025 it is estimated that this number will exceed four million. *Diabetic peripheral neuropathy* (DPN) is one of the most common long-term complications of diabetes and is the main initiating factor for foot ulceration, Charcot's neuroarthropathy and lower extremity amputation. Around 50% of patients with diabetes may suffer from DPN [1] resulting in pain, foot ulcers, blindness etc. It is estimated that about 16.2% of people with diabetes are affected by chronic painful neuropathy [3]. As 80% of amputations are preceded by foot ulceration, an effective means of detecting and treating neuropathy would have a major medical, social and economic impact. The accurate detection and quantification of DPN are important for defining at-risk patients, anticipating deterioration, and assessing new therapies. Current methods of diagnosis are unsatisfactory, being highly invasive (skin biopsy) or lacking sensitivity, require expert assessment or focus only on large nerve fibres whereas the earliest signs of neuropathy are likely to be found among small nerve fibres.

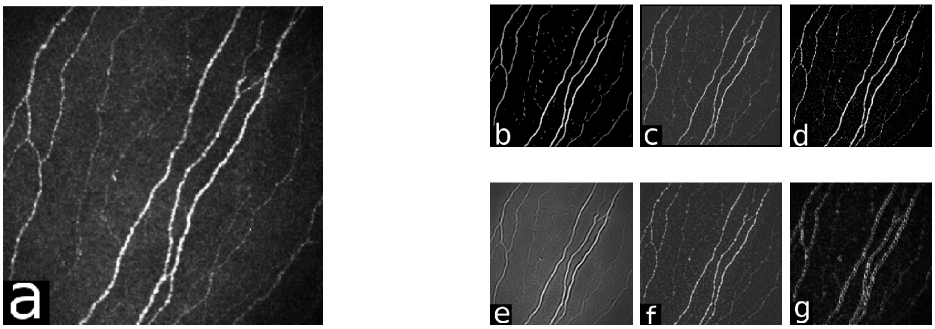

Figure 1: An illustration of the methods' responses. (a) the CCM image, (b) Dual-model, (c) LinOp, (d) Hessian, (e) 2D Gabor, (f) Monogenic and (g) DTCWT.

However, recent research [10] using Corneal Confocal Microscopy (CCM) suggests that this non-invasive, and hence reiterative, test might be an ideal surrogate endpoint for human diabetic neuropathy. These studies demonstrate that measurements made by CCM accurately quantify corneal nerve fibre morphology. The measurements reflect the severity of DPN and relate to the extent of intra-epidermal nerve fibre loss seen in skin biopsy. However, the major limitation preventing extension of this technique to wider clinical practice is that analysis of the images using interactive image analysis is highly labour-intensive and requires considerable expertise to quantify nerve fibre pathology. To be clinically useful as a diagnostic tool, it is essential that the measurements be extracted automatically.

2 Corneal Nerve Fibre Detection

The first critical stage in analysis of CCM images (an example is shown in figure 1(a)) is the detection of nerve fibres. The nerve fibres often show poor contrast in the relatively noisy images. These captured images of nerve fibre structures could suffer from several types of corruption due to some acquisition conditions, and nerve fibres may appear faint due to their small size or being only partly in the focus plane. Therefore, a nerve fibre contrast enhancement algorithm is needed to exploit the linear structure of the nerve fibres and distinguish them from the background noise. All the methods described in this section are capable of providing this enhancement. The problem of extracting nerve fibres from CCM images has a superficial similarity to other, more widely investigated, applications, such as detection of blood-vessels in retinal images.

A method of linear structure detection (Line Operator - LinOp), originally developed for detection of asbestos fibres has also been shown to be effective in detecting ducts in mammograms [12]. LinOp exploits the linear nature of the structures to enhance their contrast by computing the average intensity of pixels lying on a line passing through the reference pixel for multiple orientations and scales. In a a preliminary study [2], we use the 2D Gabor filter [8] to detect nerve fibres in CCM images. The filter is a band-pass filter that consists of a sinusoidal plane wave modulated by a Gaussian envelope and tuned to the local orientation and frequency of nerve fibres. Frangi *et al.* [6] used a multi-scale decomposition of the Hessian matrix to detect and measure blood vessels in Digital Subtraction Angiography images. They derived a discriminant function based on the eigenvalues and eigenvectors, which has maximum response for tube-like structures. The Dual-Tree Complex Wavelet Transform (DTCWT) [9] is an extension of the Discrete Wavelet Transform (DWT), which provides a sparse representation and characterisation of structures and texture of the image at multi-resolutions. The DTCWT utilises two DWT decompositions (trees) with specifically selected filters, giving it the properties of approximate shift-invariance and good directionality. The Monogenic signal [5] (a variant of a 2D analytic signal) is an extension of the analytic signal using quaternionic algebra in an attempt to generalise the method so it is capable of analysing intrinsically 2D signals e.g. structures within images. The Monogenic

signal is based on the Riesz transform, which is a 2D generalization of the Hilbert transform used in the conventional analytic signal.

3 Dual-Model Nerve fibre Detection

This paper presents a dual-model algorithm for automatic detection and measurement of nerve fibres in CCM images. Using a 2D Gabor wavelet and a Gaussian envelope, the dual-model of foreground (nerve fibres) and background is constructed and applied to the original CCM image. The foreground model $\mathscr{M}_{\mathscr{F}}$ is an an even-symmetric and real-valued Gabor [8] wavelet and the background model $\mathscr{M}_{\mathscr{B}}$ is a two-dimensional Gaussian envelope.

$$\mathscr{M}_{\mathscr{F}}^{(x_\theta, y_\theta)} = \cos\left(\frac{2\pi}{\lambda}x_\theta + \phi\right) e^{\left\{-\frac{1}{2}\left(\frac{x_\theta^2}{\sigma_x^2} + \frac{\gamma^2 y_\theta^2}{\sigma_y^2}\right)\right\}} \tag{1}$$

$$\mathscr{M}_{\mathscr{B}}^{(x_\theta, y_\theta)} = \alpha e^{\left\{-\frac{1}{2}\left(\frac{x_\theta^2}{\sigma_x^2} + \frac{\gamma^2 y_\theta^2}{\sigma_y^2}\right)\right\}} \tag{2}$$

The x and y axes of the dual-model coordinate frame $x_\theta = x\cos\theta + y\sin\theta$ and $y_\theta = -x\sin\theta + y\cos\theta$ are defined by a rotation of θ, which is the dominant orientation of the nerve fibres in a particular region within the image (the method for estimating the local orientation is described below). This dual-model is used to generate the positive response $\mathscr{R}_{\mathscr{P}} = \mathscr{M}_{\mathscr{F}} + \mathscr{M}_{\mathscr{B}}$ and the negative response $\mathscr{R}_{\mathscr{N}} = \mathscr{M}_{\mathscr{F}} - \mathscr{M}_{\mathscr{B}}$ that are applied to the original CCM image and can be represented as in equations (3) and (4) respectively.

$$\mathscr{R}_{\mathscr{P}}^{(x_\theta, y_\theta)} = \left[\cos\left(\frac{2\pi}{\lambda}x_\theta + \phi\right) + \alpha\right] e^{\left\{-\frac{1}{2}\left(\frac{x_\theta^2}{\sigma_x^2} + \frac{\gamma^2 y_\theta^2}{\sigma_y^2}\right)\right\}} \tag{3}$$

$$\mathscr{R}_{\mathscr{N}}^{(x_\theta, y_\theta)} = \left[\cos\left(\frac{2\pi}{\lambda}x_\theta + \phi\right) - \alpha\right] e^{\left\{-\frac{1}{2}\left(\frac{x_\theta^2}{\sigma_x^2} + \frac{\gamma^2 y_\theta^2}{\sigma_y^2}\right)\right\}} \tag{4}$$

The equations of $\mathscr{R}_{\mathscr{P}}$ and $\mathscr{R}_{\mathscr{N}}$ assume that the Gaussian envelope of both responses are identical i.e. they have the same variances $\sigma^2_{(x,y)}$ and the same aspect ratio γ. The magnitude of the Gaussian envelope α defines the threshold in which a nerve fibre can be distinguished from the background image. The value of α can be set empirically to control sensitivity and accuracy of detection. The wavelength λ defines the frequency band of the information to be detected in the CCM image. Its value might be computed for a subregion within the image that has significant variability of nerve fibre width. However for simplicity, λ is chosen to be a global estimate of the entire image based on empirical results.

$$g^{(i,j)} = \frac{\left\langle f_\omega^{(i,j)}, \mathscr{R}_{\mathscr{P}} \right\rangle}{1 + e^{\left(-2k\left\langle f_\omega^{(i,j)}, \mathscr{R}_{\mathscr{N}} \right\rangle\right)}} \tag{5}$$

The positive and negative responses are obtained at each pixel by taking the dot product of each with the local neighbourhood of width ω around the pixel $f^{(i,j)}$. They are combined using a logistic function (equation (5)), which adjusts the model to suit the local neighbourhood characteristics, producing the modified image value, $g^{(i,j)}$. In this way, structures that are oriented in the dominant direction are enhanced, while anything else is diminished, increasing the contrast between nerve fibres and noisy background and reducing the noise around the nerve fibre (figure 1(b)). The sharpness of the transition of the enhanced image value at a particular pixel $g^{(i,j)}$ is controlled by k. A larger k amounts to a sharper transition.

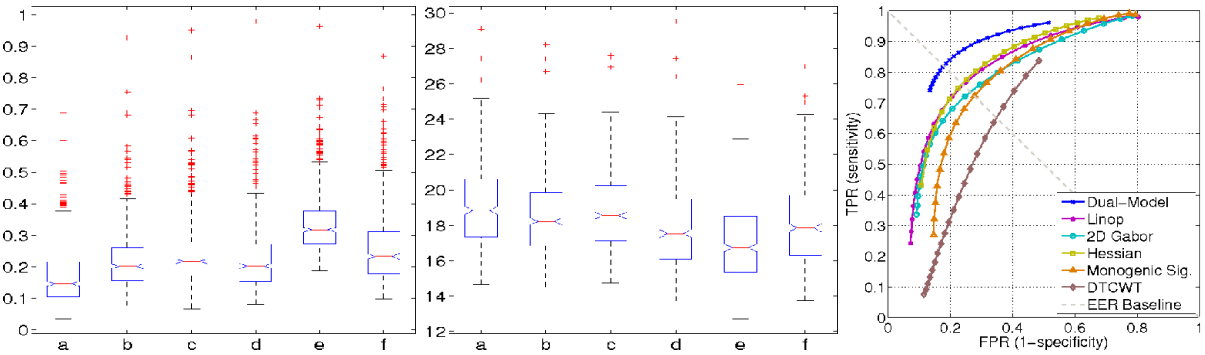

Figure 2: From left to right, the box-plots of the EER and the PSNR are shown for all methods. The ROC curves are presented at the far right. The box-plots indicate the upper and the lower quartiles as well as the median (the bar) of the EER and PSNR values respectively; whiskers show the extent of the rest of the data while crosses indicate outliers for (a) dual-model, (b) LinOp, (c) 2D Gabor, (d) Hessian, (e) DTCWT and (f) Monogenic.

	Dual-Model	LinOp [12]	2D Gabor [2, 8]	Hessian [6]	DTCWT [9]	Monog. [5]
$EER_{[\%]}$	17.79± 10.58	22.65± 10.76	24.15± 10.74	23.14± 11.53	34.17± 10.43	26.50± 12.58
$PSNR_{[dB]}$	19.08± 2.16	18.51± 2.09	18.80± 2.11	17.93± 2.27	17.00± 2.23	18.11± 2.20

Table 1: A comparison of mean EER and PSNR and their standard deviations.

In CCM images, the nerve fibres flow in locally consistent orientations everywhere. In addition, there is a global orientation that dominates the general flow. This orientation field describes the coarse structure of nerve fibres. Using the least mean square (LMS) algorithm [7], the local orientation is estimated in the block centred at certain pixel. Since the orientations vary at a slow rate, a low-pass Gaussian filter is applied globally in order to further reduce errors at near-nerve fibre and non-nerve fibre regions. The LMS produces a stable smooth orientation field in the region of the nerve fibres; however when applied on the background of the image, i.e. between fibres, the estimate is dominated by noise due to the lack of structure and uniform direction.

4 Experimental Results and Analysis

The evaluation has been conducted on a database of 525 CCM images captured using the HRT-III microscope from 69 subjects (20 controls and 49 diabetic patients). The resolution is $1.0417\mu m$ and the field of view is $400 \times 400\mu m^2$ of the cornea. For each individual, several fields of view are selected manually from near the centre of the cornea that show recognisable nerve fibres.

The performance of all methods is obtained by validating the extracted nerve fibres in comparison with an expert manual delineation.Only the raw response of each method is taken into account without any further post-processing operations or shade correction methods as shown in figure 1. Binary images are obtained by a simple uniform thresholding operation that is followed by a thinning operation to achieve a one-pixel-wide skeleton image. A tolerance of $\pm 3.141\mu m$ (3 pixels) was allowed in determining coincidence between the ground-truth and the detected nerve fibres.

The equal-error rate (EER) and peak signal to noise ratio (PSNR) values for all the methods are presented in the box-plots in figure 2 and table 1. Each data point in figure 2 corresponds to the evaluation on one of the 525 CCM images in the database. The dual-model shows lower EER and higher PSNR than all other methods (table 1). These improvements are statistically significant ($p \approx 0$ using three different non-parametric tests). The table also shows that the standard deviations of both EER and PSNR are low for the dual-model, which

indicates a more stable and robust behaviour. The closest competitor is LinOp. The methods designed for linear structures perform rather better on this test than the more generic DTCWT and Monogenic signal methods. The superior performance of the dual-model is borne out by the ROC curves of figure 2, in which the dual model shows improved detection at all operation points.

5 Conclusion

The analysis of CCM images requires the identification of fibre-like structures with low contrast in noisy images. This is a requirement shared by a number of imaging applications in biology, medicine and other fields. A number of methods have been applied in these applications, and we have compared some of these, and more generic methods with a dual-model detection algorithm devised for this study. The comparison used a large set of images with manual ground truth. In terms of both error-rates (pixel misclassification) and signal-to-noise ratio, the dual model achieved highest performance. It seems reasonable to propose that this filter is likely to prove equally useful in applications of a similar nature.

References

[1] Andrew J.M. Boulton. Management of Diabetic Peripheral Neuropathy. *Clinical Diabetes*, 23 (1):9–15, 2005.

[2] M. A. Dabbah, J. Graham, M. Tavakoli, Y. Petropoulos, and R. A. Malik. Nerve fibre extraction in confocal corneal microscopy images for human diabetic neuropathy detection using gabor filters. In *Medical Image Understanding and Analysis (MIUA)*, pages 254–258, July 2009.

[3] C. Daousi, I. A. MacFarlane, A. Woodward, T. J. Nurmikko, P. E. Bundred, and S. J. Benbow. Chronic painful peripheral neuropathy in an urban community: a controlled comparison of people with and without diabetes. *Diabetic Medicine*, 21(9):976–982, 2004.

[4] DiabetesUK. Diabetes in the uk 2010: Key statistics on diabetes. *http://www.diabetes.org.uk/*, 2010.

[5] M. Felsberg and G. Sommer. The monogenic signal. *IEEE Transactions on Signal Processing*, 49(12):3136–3144, Dec 2001.

[6] Alejandro F. Frangi, Wiro J. Niessen, Koen L. Vincken, and Max A. Viergever. Multiscale vessel enhancement filtering. In *Medical Image Computing and Computer-Assisted Interventation (MICCAI)*, pages 130–137, July 1998.

[7] Lin Hong, Yifei Wan, and A. Jain. Fingerprint image enhancement: algorithm and performance evaluation. *IEEE Transactions on Pattern Analysis and Machine Intelligence*, 20(8):777–789, Aug 1998.

[8] Anil K. Jain and Farshid Farrokhnia. Unsupervised texture segmentation using gabor filters. *Pattern Recognition*, 24(12):1167–1186, 1991.

[9] Nick Kingsbury. Complex wavelets for shift invariant analysis and filtering of signals. *Applied and Computational Harmonic Analysis*, 10(3):234 – 253, 2001.

[10] R A Malik, P Kallinikos, C A Abbott, C H M van Schie, P Morgan, N Efron, and A J M Boulton. Corneal confocal microscopy: a non-invasive surrogate of nerve fibre damage and repair in diabetic patients. *Diabetologia*, 46(5):683–688, 2003.

[11] J.E. Shaw, R.A. Sicree, and P.Z. Zimmet. Global estimates of the prevalence of diabetes for 2010 and 2030. *Diabetes Research and Clinical Practice*, 87:4–14, 2010.

[12] R Zwiggelaar, SM Astley, CRM Boggis, and CJ Taylor. Linear structures in mammographic images: Detection and classification. *IEEE Transactions on Medical Imaging*, 23(9):1077–1086, Sep. 2004.